Inorg. Chem. **2002**, *41*, 3137–3145

Substitution Reactions of $[Ru(dppe)(CO)(H_2O)_3][OTf]_2$

Matthew D. Hargreaves, Mary F. Mahon, and Michael K. Whittlesey*

Department of Chemistry, University of Bath, Claverton Down, Bath BA2 7AY, U.K.

Received January 9, 2002

The labile nature of the coordinated water ligands in the organometallic aqua complex $[Ru(dppe)(CO)(H_2O)_3][OTf]_2$ (**1**) (dppe = $Ph_2PCH_2CH_2PPh_2$; OTf = OSO_2CF_3) has been investigated through substitution reactions with a range of incoming ligands. Dissolution of **1** in acetonitrile or dimethyl sulfoxide results in the facile displacement of all three waters to give $[Ru(dppe)(CO)(CH_3CN)_3][OTf]_2$ (**2**) and $[Ru(dppe)(CO)(DMSO)_3][OTf]_2$ (**3**), respectively. Similarly, **1** reacts with Me_3CNC to afford $[Ru(dppe)(CO)(CNCMe_3)_3][OTf]_2$ (**4**). Addition of 1 equiv of 2,2′-bipyridyl (bpy) or 4,4′-dimethyl-2,2′-bipyridyl (Me_2bpy) to acetone/water solutions of **1** initially yields $[Ru(dppe)(CO)(H_2O)(bpy)][OTf]_2$ (**5a**) and $[Ru(dppe)(CO)(H_2O)(Me_2bpy)][OTf]_2$ (**6a**), in which the coordinated water lies trans to CO. Compounds **5a** and **6a** rapidly rearrange to isomeric species (**5b**, **6b**) in which the ligated water is trans to dppe. Further reactivity has been demonstrated for **6b**, which, upon dissolution in $CDCl_3$, loses water and coordinates a triflate anion to afford $[Ru(dppe)(CO)(OTf)(Me_2bpy)][OTf]$ (**7**). Reaction of **1** with $CH_3CH_2CH_2SH$ gives the dinuclear bridging thiolate complex $[\{(dppe)Ru(CO)\}_2(\mu\text{-}SCH_2CH_2CH_3)_3][OTf]$ (**8**). The reaction of **1** with CO in acetone/water is slow and yields the cationic hydride complex $[Ru(dppe)(CO)_3H][OTf]$ (**9**) via a water gas shift reaction. Moreover, the same mechanism can also be used to account for the previously reported synthesis of **1** upon reaction of $Ru(dppe)(CO)_2(OTf)_2$ with water (*Organometallics* **1999**, *18*, 4068).

Introduction

Water is ubiquitous as a ligand in coordination chemistry. In contrast, organometallic aqua complexes are far less common largely because the presence of both soft ligands such as phosphines and CO and harder oxygen donors such as water is thought of as being incompatible. In recent years, however, considerable interest has developed into the study of aqueous organometallic chemistry[1] due to the potential applications of water-soluble complexes in organic synthesis,[2] biphasic and homogeneous catalysis,[3] and medicinal chemistry.[4] Of all of the late transition metals, aqua complexes of ruthenium(II) have attracted the most attention since the

* Corresponding author. E-mail: chsmkw@bath.ac.uk.

(1) (a) Cornils, B.; Herrmann, W. A. *Aqueous Phase Organometallic Catalysis*; Wiley-VCH: Weinheim, 1998. (b) Joó, F.; Kathó, A. *J. Mol. Catal.* **1997**, *116*, 3. (c) Richens, D. T. *The Chemistry of Aqua Ions*; Wiley: Chichester, 1997. (d) Roundhill, D. M. *Adv. Organomet. Chem.* **1995**, *38*, 155. (e) Kölle, U.; Görissen, R.; Wagner, T. *Chem. Ber*. **1995**, *128*, 911. (f) Eisen, M. S.; Haskel, A.; Chen, H.; Olmstead, M. M.; Smith, D. P.; Maestre, M. F.; Fish, R. H. *Organometallics* **1995**, *14*, 2806. (g) Svetlanova-Larsen, A.; Zoch, C. R.; Hubbard, J. L. *Organometallics* **1996**, *15*, 3076. (h) Caraiati, E.; Lucenti, E.; Pizzotti, M.; Roberto, D.; Ugo, R. *Organometallics* **1996**, *15*, 4122. (i) Takahashi, Y.; Akita, M.; Hikichi, S.; Moro-oka, Y. *Inorg. Chem*. **1998**, *37*, 3186. (j) Leung, W.-H.; Chan, E. Y. Y.; Wong, W.-T. *Inorg. Chem*. **1999**, *38*, 136. (k) Balzarek, C.; Weakley, T. J. R.; Kuo, L. Y.; Tyler, D. R. *Organometallics* **2000**, *19*, 2927. (l) Akita, M.; Takahashi, Y.; Hikichi, S.; Moro-oka, Y. *Inorg. Chem*. **2001**, *40*, 169. (m) Hughes, R. P.; Lindner, D. C.; Smith, J. M.; Zhang, D.; Incarvito, C. D.; Lam, K.-C.; Liable-Sands, L. M.; Sommer, R. D.; Rheingold, A. L. *J. Chem. Soc., Dalton Trans*. **2001**, 2270. (n) Poth, T.; Paulus, H.; Elias, H.; Dücker-Benfer, C.; van Eldik, R. *Eur. J. Inorg. Chem.* **2001**, 1361.

(2) (a) Laurenczy, G.; Merbach, A. E. *J. Chem. Soc., Chem. Commun.* **1993**, 187. (b) Le, T. X.; Merola, J. S. *Organometallics* **1993**, *12*, 3798. (c) Aebischer, N.; Frey, U.; Merbach, A. E. *Chem. Commun*. **1998**, 2303. (d) Balzarek, C.; Tyler, D. R. *Angew. Chem., Int. Ed*. **1999**, *38*, 2406. (e) Takahashi, Y.; Kikichi, S.; Akita, M.; Moro-oka, Y. *Chem. Commun*. **1999**, 1491. (f) Balzarek, C.; Weakley, T. J. R.; Tyler, D. R. *J. Am. Chem. Soc.* **2000**, *122*, 9427. (g) Breno, K. L.; Tyler, D. R. *Organometallics* **2001**, *20*, 3864.

(3) (a) McGrath, D. V.; Grubbs, R. H.; Ziller, J. W. *J. Am. Chem. Soc*. **1991**, *113*, 3611. (b) Hillmyer, M. A.; Lepetit, C.; McGrath, D. V.; Novak, B. M.; Grubbs, R. H. *Macromolecules* **1992**, *25*, 3345. (c) Wang, L.; Lu, R. S.; Bau, R.; Flood, T. C. *J. Am. Chem. Soc*. **1993**, *115*, 6999. (d) Ogo, S.; Makihara, N.; Watanabe, Y. *Organometallics* **1999**, *18*, 5470. (e) Verspui, G.; Schanssema, F.; Sheldon, R. A. *Angew. Chem., Int. Ed.* **2000**, *39*, 804. (f) Makihara, N.; Ogo, S.; Watanabe, Y. *Organometallics* **2001**, *20*, 497. (g) Ogo, S.; Makihara, N.; Kaneko, Y.; Watanabe, Y. *Organometallics* **2001**, *20*, 4903.

(4) (a) Alberto, R.; Egli, A.; Abram, U.; Hegetschweiler, K.; Gramlich, V.; Schubiger, P. A. *J. Chem. Soc., Dalton Trans*. **1994**, 2815. (b) Egli, A.; Hegetschweiler, K.; Alberto, R.; Abram, U.; Schibli, R.; Hedinger, R.; Gramlich, V.; Kissner, R.; Schubiger, P. A. *Organometallics* **1997**, *17*, 1833. (c) Alberto, R.; Schibli, R.; Egli, A.; Schubiger, A. P.; Abram, U.; Kaden, T. A. *J. Am. Chem. Soc.* **1998**, *120*, 7987. (d) Fish, R. H. *Coord. Chem. Rev*. **1999**, *185/186*, 569. (e) Aebischer, N.; Schibli, R.; Alberto, R.; Merbach, A. E. *Angew. Chem., Int. Ed.* **2000**, *39*, 254.

10.1021/ic020029z CCC: $22.00
Published on Web 05/16/2002

+2 oxidation state of this metal has been shown to exhibit a strong binding affinity for both water and π acid ligands such as alkenes.[5]

The presence of "organometallic" ligands can have remarkable effects on the substitution patterns of aqua complexes. Kinetic measurements using ^{17}O NMR spectroscopy have revealed that the relative rates of water exchange in $[(\eta^6\text{-}C_6H_6)Ru(H_2O)_3]^{2+}$, $[Ru(H_2O)_5(CO)]^{2+}$, and $[Ru(H_2O)_6]^{2+}$ are in the ratio 640:2.5:1. Merbach and coworkers have reported extensive studies on the rates of water exchange and displacement in $[Ru(H_2O)_5L]^{2+}$, $[Ru(H_2O)_4L_2]^{2+}$ (L = C_2H_4, CO, CH_3CN, N_2), and $[(arene)Ru(H_2O)_3]^{2+}$.[6] Thus, the cationic species $[Ru(H_2O)_5L]^{2+}$ shows different rates of exchange for water ligands in the equatorial and axial positions and attempts have been made to correlate this reactivity to the labilizing cis and trans effects of both the ancilliary ligands, L, and water itself. While trans effects are comparatively well understood for square planar complexes, much less is known about similar effects in octahedral complexes,[7] largely because there are a greater number of variables to consider in the latter including the metal center, nature of the leaving groups, and mechanisms of reaction (I_d, I_a, etc.).

We have recently reported the formation of the carbonyl aqua complex $[Ru(dppe)(CO)(H_2O)_3]^{2+}$ (**1**) upon addition of water to $[Ru(dppe)(CO)_2(OTf)_2]$.[8] The X-ray structure determination of **1** shows that the molecule contains a *fac*-$[Ru(OH_2)_3]^{2+}$ moiety, thus affording the possibility of studying the lability of the coordinated waters (two trans to P, one trans to CO) with a range of incoming ligands L. Prior to embarking on kinetic studies on the reactivity of **1**, we have sought to establish the substitution chemistry of **1** with a range of unidentate, bidentate, and potentially bridging groups. We now report that both mononuclear and binuclear ruthenium(II) complexes can be formed upon substitution of one, two, or all three water ligands. In many of these reactions, the products have been characterized by X-ray crystallography, which has provided evidence for hydrogen bonding interactions in the solid state.

Experimental Section

General Comments. All reactions were carried out using standard Schlenk and high vacuum techniques. Water was doubly distilled and degassed prior to use, while CH_2Cl_2 was distilled from P_2O_5. Deuterated solvents (Goss) were dried over CaH_2 ($CDCl_3$ and CD_2C1_2); $(CD_3)_2CO$ and CD_3CN were freeze−pump−thaw degassed while D_2O was degassed by bubbling with argon. Silver triflate (Lancaster) was handled in a nitrogen-filled glovebox. 2,2′-Bipyridyl (bpy) and 4,4′-dimethyl-2,2′-bipyridyl (Me_2bpy) (Aldrich), propanethiol (Aldrich), CO (BOC, 99.9%), and ^{13}CO (Promochem, 99%) were used as received. $Ru(dppe)(CO)_2(OTf)_2$ and $Ru(dppe)(CO)_3$ were prepared as described in the literature.[8,9] ^1H NMR spectra were recorded on Bruker AVANCE 300 or Varian Mercury 400 MHz NMR spectrometers and referenced to residual protio solvent resonances (acetone δ 2.05, chloroform δ 7.27, dimethyl sulfoxide (DMSO) δ 2.54). All spectra were recorded in mixtures of acetone-d_6 and H_2O unless otherwise stated. $^{31}P\{^1H\}$ and ^{19}F NMR chemical shifts were referenced externally to 85% H_3PO_4 and $CFCl_3$, respectively (both at δ 0.00). $^{13}C\{^1H\}$ NMR spectra were referenced to acetone-d_6 at δ 30.6. ^1H COSY, $^1H-^{13}C$ HMQC, and HMBC experiments were performed on the AVANCE spectrometer using standard Bruker pulse sequences. Only the most pertinent NMR data are reported with peak positions given in parts per million and coupling constants in hertz. IR spectra reported in cm^{-1} were recorded on a Nicolet Protégé 460 FTIR spectrometer. Elemental analyses were performed at the University of Bath.

$[Ru(dppe)(CO)(H_2O)_3][OTf]_2$ (1). To a solution of $Ru(dppe)(CO)_2(OTf)_2$ (70 mg, 0.082 mmol) in CH_2Cl_2 (5 mL) was added 10 equiv of water (15 μL, 0.83 mmol). Pale Yellow crystals of **1** slowly crystallized from the solution after 2 days at 5 °C (59.5 mg, yield 85%). ^1H NMR (293 K): 7.98−7.90 (6H, m, PC_6H_5), 7.55−7.50 (10H, m, PC_6H_5), 7.37 (2H, m, PC_6H_5), 6.94 (2H, m, PC_6H_5), 3.49−3.43 (2H, m, PCH_2), 3.14−3.08 (2H, m, PCH_2). $^{31}P\{^1H\}$: 66.5 (s). ^{19}F: −79.20 (s). $^{13}C\{^1H\}$: 198.3 (t, J_{CP} = 17.9, CO). Larger quantities of **1** were more easily prepared by addition of AgOTf (272 mg, 1.06 mmol) to a solution of all *cis*-$Ru(dppe)(CO)_2Cl_2$ (302 mg, 0.48 mmol) in 15 mL of CH_2Cl_2 followed immediately by water (86 μL, 4.77 mmol). After the mixture was stirred for 90 min with the total exclusion of light, the precipitate of AgCl was removed by filtration and the pale yellow filtrate concentrated by half. Crystals of **1** slowly precipitated out of solution (130 mg, yield 43%).

$[Ru(dppe)(CO)(CH_3CN)_3][OTf]_2$ (2). A sample of **1** (10 mg, 0.011 mmol) was placed in a J. Young's resealable NMR tube and dissolved in CD_3CN (0.6 mL). The $^{31}P\{^1H\}$ NMR spectrum showed immediate conversion to **2**. Removal of the solvent and recrystallization of the residue from chloroform/acetonitrile Et_2O gave **2** in analytically pure form. ^1H NMR (acetone-d_6, 293 K): 2.78 (s, 6H, CH_3CN), 2.00 (s, 3H, CH_3CN). $^{31}P\{^1H\}(CD_3CN)$: 62.3 (s). $^{19}F(CD_3CN)$: −79.20 (s). $^{13}C\{^1H\}(CD_3CN)$: 194.1 (t, J_{CP} = 16.1, CO), 3.5 (s, CH_3CN), 2.2 (s, CH_3CN). IR (Nujol): 2324 m (ν_{CN}), 2294 m (ν_{CN}), 2020 vs (ν_{CO}).

$[Ru(dppe)(CO)(Me_2SO)_3][OTf]_2$ (3). A sample of **1** (10 mg, 0.011 mmol) was placed in a J. Young's resealable NMR tube and dissolved in degassed DMSO (0.6 mL). The $^{31}P\{^1H\}$ NMR spectrum showed immediate conversion to **3**. Removal of the solvent and recrystallization of the residue from acetone/DMSO/Et_2O gave **3** in analytically pure form (8 mg, 75% yield). ^1H NMR (DMSO-d_6, 293 K): 3.34 (s, 12H, Me_2SO), 2.99 (s, 6H, Me_2SO). $^{31}P\{^1H\}$: 64.7 (s). ^{19}F: −79.33 (s). $^{13}C\{^1H\}$: 199.1 (t, J_{CP} = 17.4, CO). IR (KBr): 1973 vs (ν_{CO}).

$[Ru(dppe)(CO)(CNCMe_3)_3][OTf]_2$ (4). Addition of 81 μL of Me_3CNC (0. 72 mmol) to an acetone-d_6/H_2O solution of **1** (126 mg, 0.14 mmol) gave an immediate color change from pale yellow to colorless with the appearance of a new resonance in the $^{31}P\{^1H\}$ NMR spectrum at δ 54.8. This species fully converted to a

(5) (a) Kölle, U. *Coord. Chem. Rev.* **1994**, *135/136*, 623. (b) For a very recent overview of aqueous ruthenium chemistry, see: Grundler, P. V.; Laurenczy, G.; Merbach, A. E. *Helv. Chim. Acta* **2001**, *84*, 2854.
(6) (a) Dadci, L.; Elias, H.; Frey, U.; Hörnig, A.; Kölle, U.; Merbach, A. E.; Paulus, H.; Schneider J. S. *Inorg. Chem.* **1995**, *34*, 306. (b) Aebischer, N.; Sidorenkova, E.; Ravera, M.; Laurenczy, G.; Osella, D.; Weber, J.; Merbach, A. E. *Inorg. Chem.* **1997**, *36*, 6009. (c) Aebischer, N.; Churlaud, R.; Dolci, L.; Frey, U.; Merbach, A. E. *Inorg. Chem.* **1998**, *37*, 5915. (d) Cayemittes, S.; Poth, T.; Fernandez, M. J.; Lye, P. G.; Becker, M.; Elias, H.; Merbach, A. E. *Inorg. Chem.* **1999**, *38*, 4309. (e) Meier, U. C.; Scopelliti, R.; Solari, E.; Merbach, A. E. *Inorg. Chem.* **2000**, *39*, 3816.
(7) Coe, B. J.; Glenwright, S. J. *Coord. Chem. Rev.* **2000**, *203*, 5.
(8) Mahon, M. F.; Whittlesey, M. K.; Wood, P. T. *Organometallics* **1999**, *18*, 4068.
(9) Bunten, K. A.; Farrar, D. H.; Poë, A. J.; Lough, A. J. *Organometallics* **2000**, *19*, 3674.

Table 1. Experimental Data for the X-ray Diffraction Studies of Compounds **2**, **3**, **4**, **7**, and **8**

	2	**3**	**4**	**7**	**8**
empirical formula	$C_{37}H_{35}Cl_6F_6N_3O_7P_2RuS_2$	$C_{38}H_{48}F_6O_{11}P_2RuS_5$	$C_{45.50}H_{54}F_6N_3O_{7.50}P_2RuS_2$	$C_{41}H_{36}F_6N_2O_7P_2RuS_2$	$C_{67}H_{75}F_3O_6P_4Ru_2S_4$
formula weight	1187.51	1118.07	1104.05	1009.85	1490.55
temp/K	170(2)	150(2)	150(2)	170(2)	170(2)
crystal system	monoclinic	orthorhombic	monoclinic	monoclinic	triclinic
space group	$P2_1/n$	$P2_12_12_1$	$P2_1/n$	$P2_1/c$	$P\bar{1}$
a/Å	12.2606(3)	11.5396(1)	12.1103(1)	14.2643(2)	12.655(1)
b/Å	13.8259(3)	20.2593(1)	21.9721(1)	13.7762(2)	12.998(1)
c/Å	29.5038(5)	20.4265(1)	19.6937(2)	22.1901(4)	21.065(2)
α/deg					100.982(5)
β/deg	99.587(1)		90.1040(3)	108.196(1)	92.936(5)
γ/deg					103.143(5)
U/Å^3	4931.45(18)	4775.39(5)	5240.26(7)	4143.5(1)	3296.11(5)
Z	4	4	4	4	2
crystal size/mm	0.37 × 0.20 × 0.13	0.28 × 0.25 × 0.25	0.30 × 0.20 × 0.10	0.17 × 0.13 × 0.13	0.25 × 0.20 × 0.10
θ range for data collection/deg	1.71−26.37	4.60−30.03	3.53−27.12	3.58−27.48	3.54−27.50
index ranges	$-15 \le h \le 15$; $-16 \le k \le 17$; $-32 \le l \le 34$	$-15 \le h \le 16$; $-28 \le k \le 27$; $-28 \le l \le 28$	$-15 \le h \le 13$; $-27 \le k \le 28$; $-25 \le l \le 25$	$0 \le h \le 18$; $-17 \le k \le 17$; $-28 \le l \le 27$	$0 \le h \le 16$; $-16 \le k \le 16$; $-27 \le l \le 27$
reflns collected	20 389	92 137	82 263	56 381	37 510
independent reflns	9 648 [R(int) = 0.0329]	13 879 [R(int) = 0.0377]	11 508 [R(int) = 0.0566]	94 67 [R(int) = 0.0468]	14 940 [R(int) = 0.0297]
data/restraints/params	9 648/15/609	13 879/0/596	11 508/3/635	94 67/0/551	14 940/0/776
final R1, wR2 [$I > 2\sigma(I)$]	0.0383, 0.1042	0.0337, 0.0749	0.0504, 0.1254	0.0332, 0.0934	0.0308, 0.0758
final R1, wR2 (all data)	0.0541, 0.1191	0.0350, 0.0743	0.0580, 0.1312	0.0428, 0.1006	0.0345, 0.0786

second product at δ 52.4 over 48 h. Layering with Et_2O gave white analytically pure crystals of **4** (83 mg, 66% yield). ^{1}H NMR (acetone-d_6, 293 K): 1.79 (s, 9H, Me_3CNC), 1.05 (s, 18H, Me_3CNC). ^{31}P{^{1}H}: 52.4 (s). ^{19}F: −79.35 (s). ^{13}C{^{1}H}: 190.8 (t, J_{CP} = 12.0, CO), 62.2 (s, CN*C*Me$_3$), 61.6 (s, CN*C*Me$_3$), 30.0 (s, CNC*Me*$_3$), 29.2 (s, CNC*Me*$_3$). IR (KBr): 2233 s (ν_{CN}), 2212 s (ν_{CN}), 2071 vs (ν_{CO}).

Reaction of 1 with 2,2′-Bipyridyl. A sample of **1** (25 mg, 0.029 mmol) was dissolved in acetone-d_6/H_2O, and 1 equiv of 2,2′-bipyridyl (5 mg, 0.032 mmol) was added. A new species, **5a**, formed almost immediately as shown by ^{31}P{^{1}H} NMR spectroscopy. ^{1}H NMR (273 K): 8.89 (2H, d, J_{HH} = 8.05), 8.53 (2H, d, J_{HH} = 8.05), 8.42 (2H, d, J_{HH} = 8.05), 8.07 (2H, dd, J_{HH} = 8.05). ^{31}P{^{1}H}: 58.3 (s). IR (KBr): 1996 vs (ν_{CO}). Conversion to the isomeric product **5b** was observed upon warming to room temperature for 1 h. ^{31}P{^{1}H} NMR (293 K): 64.7 (d, J_{PP} = 13.1), 52.2 (d, J_{PP} = 13.1). IR (KBr): 2000 vs (ν_{CO}).

Reaction of 1 with 4,4′-Dimethyl-2,2′-bipyridyl. The reaction of **1** with Me_2bpy was carried out in a manner similar to that above, to give **6a** almost immediately. ^{1}H NMR (258 K): 2.55 (s, Me). ^{31}P{^{1}H}: 58.6 (s). ^{19}F: −79.35 (s). ^{13}C{^{1}H}: 199.5 (t, J_{CP} = 15.6, CO), 29.2 (s, CH_3). Upon warming to room temperature for 1 h, conversion to the isomeric product **6b** was observed. ^{1}H NMR (293 K): 2.61 (s, CH_3), 2.30 (s, CH_3). ^{31}P{^{1}H}: 64.7 (d, J_{PP} = 13.1), 52.1 (d, J_{PP} = 13.1). ^{13}C{^{1}H}: 199.4 (t, J_{CP} = 16.1, CO), 21.2 (s, Me), 20.7 (s, Me). IR (KBr): 2004 vs (ν_{CO}).

[Ru(dppe)(CO)(OTf)(Me$_2$bpy)][OTf] (7). A sample of **1** (62 mg, 0.070 mmol) was dissolved in acetone/H_2O and 1 equiv of Me_2bpy (13 mg, 0.070 mmol) was added. After 1 day at room temperature, the solution was pumped to dryness and the residue redissolved in $CDCl_3$. Yellow crystals of **7** were slowly precipitated from the solution (48 mg, 68% yield). ^{1}H NMR ($CDCl_3$, 293 K): 2.61 (s, CH_3), 2.30 (s, CH_3). ^{31}P{^{1}H} (CD_2Cl_2): 67.3 (d, J_{PP} = 14.3), 51.8 (d, J_{PP} = 14.3). ^{19}F (CD_2Cl_2): −78.97 (s), −79.07 (s). IR (KBr): 2005 vs (ν_{CO}).

[{Ru(dppe)(CO)}$_2$(μ-SCH$_2$CH$_2$CH$_3$)$_3$][OTf] (8). 1-Propanethiol (38 μL, 0.42 mmol) was added to an acetone/H_2O solution of **1** (125 mg, 0.14 mmol) at room temperature to give a deep red solution. This was pumped to dryness and the residue was redissolved in acetone and layered with diethyl ether. Yellow/orange crystals formed overnight (40 mg, 32% yield). ^{1}H NMR (acetone-d_6, 293 K): 7.81 (8H, t, J_{HH} = 8.39), 7.70 (8H, t, J_{HH} = 8.39), 7.49−7.32 (24H, m), 2.65−2.85 (8H, br, PCH_2 + SCH_2), 1.29 (4H, m, C*H*$_2$CH$_3$), 1.17 (2H, m, SCH_2), 0.86 (6H, t, J_{HH} = 7.20, CH_3), 0.31 (2H, m, C*H*$_2$CH$_3$), −0.23 (3H, t, J_{HH} = 7.20, CH_3). ^{31}P{^{1}H}: 47.0 (s). ^{13}C{^{1}H}: 201.4 (t, J_{CP} = 9.6, CO). IR (KBr): 1953 vs (ν_{CO}).

[Ru(dppe)(CO)$_3$H][OTf] (9). One equivalent of HOTf (3.5 μL, 0.039 mmol) was added to a CO-saturated C_6D_6 solution of Ru(dppe)(CO)$_3$ (23 mg, 0.039 mmol) at −78 °C. The solution was thawed to room temperature with the appearance of a new singlet for **9** at δ 64.6 in the ^{31}P{^{1}H} NMR spectrum. Over 1 week at room temperature, small yellow crystals appeared, one of which was used for the structure determination. ^{1}H NMR (benzene-d_6, 293 K): −7.57 (1H, t, J_{HP} = 17.80). ^{31}P{^{1}H}: 64.6 (s). ^{13}C{^{1}H}: 192.2 (dd, J_{CP} = 76.3, 17.4, CO), 190.0 (t, J_{CP} = 7.9, CO). IR (Nujol): 2110 vs (ν_{CO}), 2062 vs (ν_{CO}), 2051 vs (ν_{CO}).

X-ray Experimental Data. Crystallographic data for compounds **2**, **3**, **4**, **7**, and **8** are summarized in Table 1. X-ray data were collected on a Nonius KappaCCD diffractometer throughout. Full matrix anisotropic refinement (SHELXL-97)[10] was implemented in the final least-squares cycles for all structures. All data were corrected for Lorentz, polarization and extinction. An absorption correction (multiscan) was applied to the data for **2** and **4** (maximum and minimum transmission factors were 1.027, 0.989 and 1.055, 0.944, respectively). Hydrogens were included at calculated positions throughout. The asymmetric unit of **2** contains two molecules of chloroform in addition to one molecule of the ruthenium salt complex. One of these solvent molecules exhibited positional disorder of the chlorine atoms in the ratio 4:1. In **3**, the phenyl group based on C2 was found to be disordered in the ratio 56:44. The ADPs pertaining to the α-carbon of each disordered portion were constrained to be similar in the final least-squares assignment. The motif in the structure of **3** also contains a molecule of acetone.

The asymmetric unit in **4** contains a molecule of acetone with half-site occupancy. Triflate based on S2 exhibits some positional

(10) Sheldrick, G. M. *Acta Crystallogr., Sect. A* **1990**, *A46*, 467−473. Sheldrick, G. M. *SHELXL-97, a computer program for crystal structure refinement*; University of Göttingen: Göttingen, Germany, 1997.

disorder approximately along the S(2)−C(44) vector which could not be successfully modeled. C−F distances were restrained to be similar in this anion. The gross structure was heavily dominated by C−H···O interactions. Disorder within the second triflate in this compound may be a consequence of the partial occupancy of the solvent, which is implicit in the C−H···O network. There is one full molecule of recrystallization (acetone) within the asymmetric unit of **8**. The highest residual electron density in this structure is in the region of C61 in the difference Fourier map, which is possibly indicative of some slight disorder within the propyl group attached to S(1).

The structure of **9** is, in many ways, a testimony to the capabilities of modern diffractometers with area detectors. Despite copious efforts, it proved impossible to grow crystals of optimum size for a structure determination in this case. Thus, data were collected on a very small crystal (0.075 × 0.075 × 0.1 mm) over a 3 day period. Structural solution proceeded readily, despite the abysmal *R*(int) and the rapid falloff in diffraction from this very small sample. The final convergence (R1 = 15.12) was hampered by disorder (approximately 60:40) of the anion, and the presence of a fragment of solvent. Metric data for the anion are poor (a consequence of the sample size), and this region of the electron density map was treated isotropically in the latter stages of refinement. The solvent was refined as a partial water molecule. We make no other claim from this structure determination other than the fact that it confirms the nature of the cation present.

In our discussions, we have highlighted and illustrated those C−H···O interactions which conform to the criteria proposed by Desiraju.[11] As methyl hydrogens were uniformly included at calculated positions, it is worth remarking that there is extensive evidence for further interactions in all structures, based on distances between carbon atoms and triflate oxygens. Crystallographic data for the structural analyses have been deposited with the Cambridge Crystallographic Data Center, CCDC no. 176745 for compound **2**, no. 176746 for compound **3**, no. 176747 for compound **4**, no. 176748 for compound **7**, and no. 176749 for compound **8**.

Results and Discussion

Attempts to find an appropriate solvent in which to study the reactions of $[Ru(dppe)(CO)(H_2O)_3][OTf]_2$, **1**, initially caused some problems. We previously noted that this complex was not stable in chlorinated solvents. Similarly, **1** does not remain intact in acetone, where it forms a number of products, believed to be mixed acetone−water adducts. However, addition of 10 equiv of water to this mixture of species in acetone solution regenerates **1** in essentially quantitative yield. Hence, unless stated, the reactions below were performed in acetone/water mixtures.

Reaction of $[Ru(dppe)(CO)(H_2O)_3][OTf]_2$ with Mondentate Ligands (L = CH_3CN, DMSO, Me_3CNC). Dissolution of **1** in the coordinating solvents CH_3CN and DMSO leads to facile substitution of all three coordinated water ligands and formation of $[Ru(dppe)(CO)(CH_3CN)_3][OTf]_2$ (**2**) and $[Ru(dppe)(CO)(DMSO)_3][OTf]_2$ (**3**), respectively, which have been characterized by NMR spectroscopy, elemental analysis, and X-ray crystallography. The $^{31}P\{^1H\}$ NMR spectra of **2** and **3** show only singlet resonances in accord with a fac arrangement of coordinating solvent molecules as in **1**. Additional confirmation of the structure

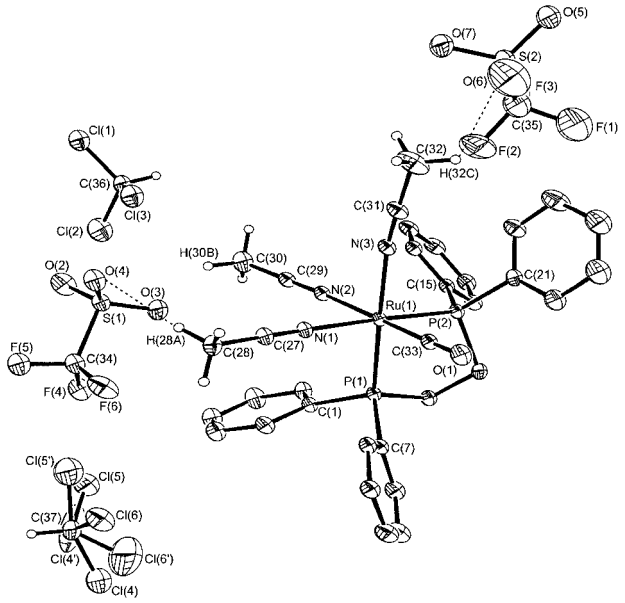

Figure 1. ORTEX diagram of $[Ru(dppe)(CO)(CH_3CN)_3][OTf]_2 \cdot 2(CHCl_3)$ (**2**). Thermal ellipsoids are shown at the 30% level.

Table 2. Selected Bond Lengths [Å] and Angles [deg] for $[Ru(dppe)(CO)(CH_3CN)_3][OTf]_2 \cdot 2(CHCl_3)$ (**2**)

Ru(1)−C(33)	1.870(3)	Ru(1)−N(2)	2.095(2)
Ru(1)−N(1)	2.109(3)	Ru(1)−N(3)	2.115(3)
Ru(1)−P(1)	2.3092(8)	Ru(1)−P(2)	2.3126(8)
C(33)−Ru(1)−N(2)	176.20(11)	C(33)−Ru(1)−N(1)	93.59(11)
N(2)−Ru(1)−N(1)	83.13(9)	C(33)−Ru(1)−N(3)	89.95(11)
N(2)−Ru(1)−N(3)	88.12(9)	N(1)−Ru(1)−N(3)	89.74(10)
C(33)−Ru(1)−P(1)	91.04(9)	N(2)−Ru(1)−P(1)	91.06(7)
N(1)Ru−(1)−P(1)	93.06(7)	N(3)−Ru(1)−P(1)	176.96(7)
C(33)−Ru(1)−P(2)	86.12(9)	N(2)−Ru(1)−P(2)	97.24(7)
N(1)−Ru(1)−P(2)	177.54(7)	N(3)−Ru(1)−P(2)	92.71(7)
P(1)−Ru(1)−P(2)	84.49(3)		

of **2** was provided by the appearance of two acetonitrile methyl resonances in both the ^1H and $^{13}C\{^1H\}$ NMR spectra (eq 1). The IR spectrum of **2** exhibits two ν_{CN} stretches[12] at

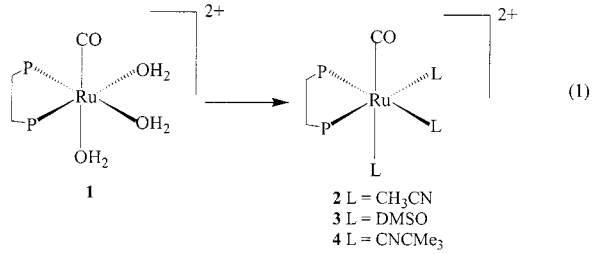

2324 and 2294 cm^{-1}, while the carbonyl band appears 30 cm^{-1} higher than that in **1**, reflecting the poorer donor ability of the acetonitrile relative to the water.

An ORTEX[13] plot representing the asymmetric unit in the X-ray structure of **2** (Figure 1) demonstrates the expected octahedral coordination geometry about the ruthenium center. Selected bond distances and angles are given in Table 2. All three Ru−N distances are similar, although the average value (2.106(3) Å) is considerably longer than average Ru−N

(11) Desiraju, G. R. *Acc. Chem. Res.* **1996**, *29*, 441.

(12) (a) Thorburn, I. S.; Rettig, S. J.; James, B. R. *J. Organomet. Chem.* **1985**, *296*, 103. (b) Bianchini, C.; Dal Santo, V.; Meli, A.; Oberhauser, W.; Psaro, R.; Vizza, F. *Organometallics* **2000**, *19*, 2433.

(13) McArdle, P. *J. Appl. Crystallogr.* **1994**, *27*, 438.

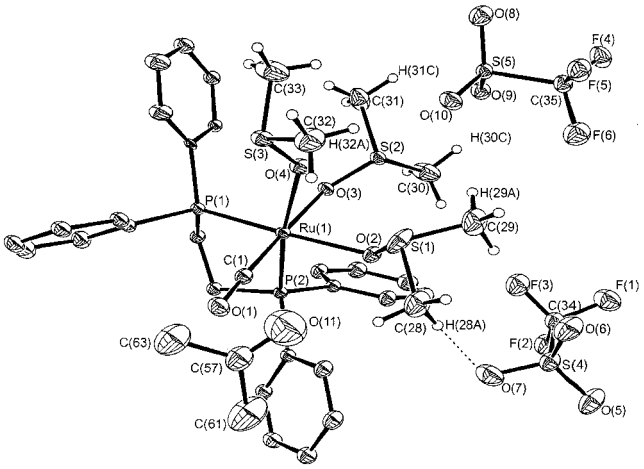

Figure 2. ORTEX diagram of [Ru(dppe)(CO)(DMSO)$_3$][OTf]$_2$ (**3**). Thermal ellipsoids are shown at the 30% level.

Table 3. Selected Bond Lengths [Å] and Angles [deg] for [Ru(dppe)(CO)(DMSO)$_3$][OTf]$_2$ (**3**)

Ru(1)−C(1)	1.831(2)	Ru(1)−O(3)	2.1353(16)
Ru(1)−O(4)	2.1524(17)	Ru(1)−O(2)	2.1808(17)
Ru(1)−P(2)	2.2866(5)	Ru(1)−P(1)	2.2941(6)
C(1)−Ru(1)−O(3)	176.18(9)	C(1)−Ru(1)−O(4)	103.35(10)
O(3)−Ru(1)−O(4)	80.47(7)	C(1)−Ru(1)−O(2)	95.20(9)
O(3)−Ru(1)−O(2)	85.21(7)	O(4)−Ru(1)−O(2)	83.48(7)
C(1)−Ru(1)−P(2)	88.07(8)	O(3)−Ru(1)−P(2)	88.12(4)
O(4)−Ru(1)−P(2)	168.00(5)	O(2)−Ru(1)−P(2)	91.93(5)
C(1)−Ru(1)−P(1)	91.06(8)	O(3)−Ru(1)−P(1)	88.33(5)
O(4)−Ru(1)−P(1)	98.25(6)	O(2)−Ru(1)−P(1)	172.94(5)
P(2)−Ru(1)−P(1)	85.03(2)		

distances found in the related ruthenium(II) complexes, $[Ru(CH_3CN)_6]^{2+}$ (2.028(1) Å),[14] $[(\eta^5\text{-}C_5H_5)Ru(CH_3CN)_3]^+$ (2.083(1) Å),[15] or $[TpRu(CH_3CN)_3]^+$ (2.045(7) Å)[16] (Tp = hydridotris(pyrazolyl)borate). This is an indication that d → π^* bonding is much less important in **2** than in these three other reported cases, a fact that is further supported by the high frequency of the ν_{CN} IR absorption bands. The crystal structure of **2** contains discrete Ru(II) cations, two triflate anions, and solvent molecules. There is evidence for C−H···O interactions using the criteria of Desiraju.[11] Thus, in the lattice array, the cation is linked to both of the $-OSO_2CF_3$ anions via weak C−H···O interactions involving hydrogens in two of the bound acetonitrile groups (C(28)−H(28A)···O(4) = 3.56 Å, C(32)−H(32B)···O(6) = 3.29 Å).

Figure 2 represents the asymmetric structure of **3**, with the relevant bond angles and distances given in Table 3. As expected in a cationic ruthenium complex, all three DMSO ligands are oxygen bound to the metal with Ru−O bond lengths in the range 2.13−2.18 Å. Although O-bonded DMSO is sterically less demanding than S-bonded DMSO,[17] the cation in **3** is still subject to steric crowding in the metal coordination sphere, which is reflected in the large Ru−O−S angles of the equatorial DMSO ligands (121.8° and 131.4°) relative to the axial bound group (118.5°). One of the triflate anions shows an interaction with the hydrogens on one of the DMSO ligands (C(28)−H(28A)···O(7) = 3.54 Å).

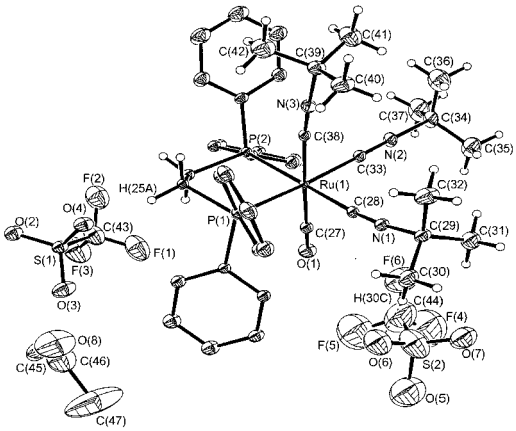

Figure 3. ORTEX diagram of [Ru(dppe)(CO)(CNCMe$_3$)$_3$][OTf]$_2$·(acetone) (**4**). Thermal ellipsoids are shown at the 30% level.

Table 4. Selected Bond Lengths [Å] and Angles [deg] for [Ru(dppe)(CO)(CNCMe$_3$)$_3$][OTf]$_2$·(acetone) (**4**)

Ru(1)−C(27)	1.937(3)	Ru(1)−C(28)	2.030(3)
Ru(1)−C(38)	2.041(3)	Ru(1)−C(33)	2.025(3)
Ru(1)−P(1)	2.3660(7)	Ru(1)−P(2)	2.3583(7)
C(27)−Ru(1)−C(33)	91.33(14)	C(27)−Ru(1)−C(38)	177.42(12)
C(33)−Ru(1)−C(28)	88.76(12)	C(28)−Ru(1)−C(38)	85.60(12)
C(33)−Ru(1)−C(38)	86.09(13)	C(33)−Ru(1)−P(2)	94.91(9)
C(27)−Ru(1)−P(2)	90.36(9)	C(38)−Ru(1)−P(2)	89.90(8)
C(28)−Ru(1)−P(2)	173.99(8)	C(33)−Ru(1)−P(1)	175.79(10)
C(27)−Ru(1)−P(1)	92.84(10)	C(38)−Ru(1)−P(1)	89.74(8)
C(28)−Ru(1)−P(1)	91.51(8)	P(2)−Ru(1)−P(1)	84.48(3)
C(27)−Ru(1)−C(28)	94.31(12)		

The reaction of **1** with excess Me_3CNC was also found to lead to substitution of all three waters by isocyanide affording [Ru(dppe)(CO)(CNCMe$_3$)$_3$][OTf]$_2$ (**4**, Figure 3). The IR spectrum displays a single carbonyl band at considerably higher frequency (2071 cm^{-1}) than found for either **2** or **3**. The bond lengths and angles in **4** are unremarkable (Table 4), although the ruthenium to carbonyl carbon bond length is significantly longer than comparable distances in either **2** or **3** (1.937(3) vs 1.870(3) and 1.831(2) Å), reflecting the competition between CO and the three other π-acceptor isocyanide ligands for electron density on the metal. Solvent of recrystallization in **4** acts solely as a lattice "cement", although one of the triflate anions displays weak hydrogen bonding interactions to hydrogen atoms in one of the equatorial $CNCMe_3$ groups (C(30)−H(30C)···O(6) = 3.48 Å, C(32)−H(32B)···O(2) = 3.40 Å).

Reaction of [Ru(dppe)(CO)(H$_2$O)$_3$][OTf]$_2$ with Bidentate Ligands (L = 2,2′-Bipyridyl (bpy) and 4,4′-Dimethyl-2,2′-bipyridyl (Me$_2$bpy)). Addition of 1 equiv of 2,2′-bipyridyl (bpy) to an acetone/water solution of **1** resulted in the rapid formation of [Ru(dppe)(CO)(H$_2$O)(bpy)][OTf]$_2$, **5a**, evidenced as a singlet in the $^{31}P\{^1H\}$ NMR spectrum, indicating that the bipyridyl ligand must be in the same plane as the bidentate phosphine. The symmetrical structure of this product was confirmed by the ^1H NMR spectrum, which showed only four pyridyl resonances. Species **5a** readily

(14) Luginbühl, W.; Ludi, A.; Raselli, A.; Bürgi, H.-B. *Acta Crystallogr., Sect. C* **1989**, *C45*, 1428.
(15) Luginbühl, W.; Zbinden, P.; Pittet, P. A.; Armbruster, T.; Bürgi, H.-B.; Merbach, A. E.; Ludi, A. *Inorg. Chem.* **1991**, *30*, 2350.
(16) Rüba, E.; Simanko, W.; Mereiter, K.; Schmid, R.; Kirchner, K. *Inorg. Chem.* **2000**, *39*, 382.
(17) (a) Alessio, E.; Bolle, M.; Milani, B.; Mestroni, G.; Faleschini, P.; Geremia, S.; Calligaris, M. *J. Chem. Soc., Dalton Trans.* **1995**, 4716. (b) Iengo, E.; Mestroni, G.; Geremia, S.; Calligaris, M.; Alessio, E. *J. Chem. Soc., Dalton Trans.* **1999**, 3361.

Scheme 1

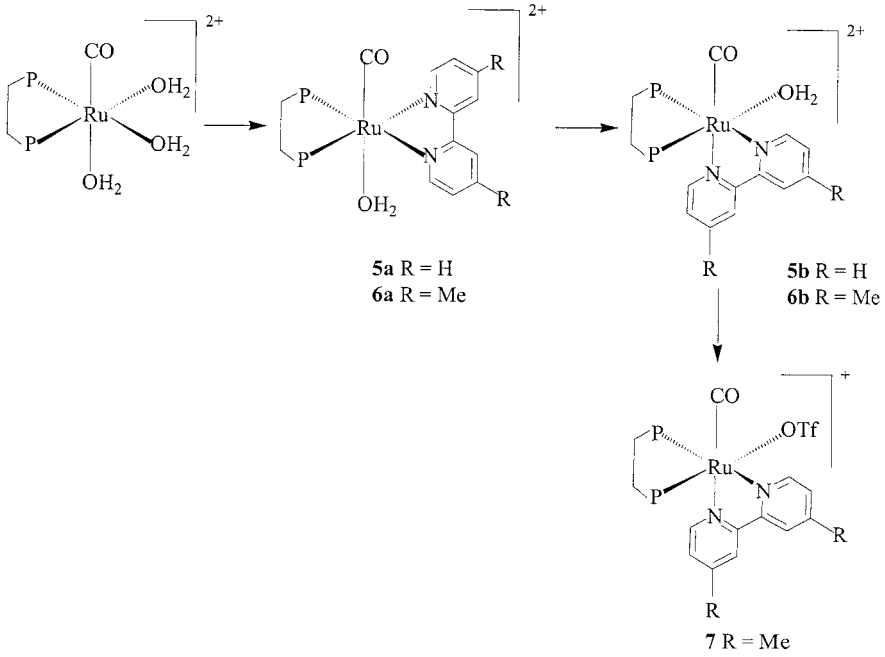

converted in ca. 1 h, at room temperature, into an isomeric product, **5b**, which displayed two doublets in the $^{31}P\{^1H\}$ NMR spectrum. Extensive overlap of pyridyl and phenyl signals in the aromatic region of the ^1H NMR spectrum prevented **5b** from being fully characterized using NMR spectroscopy. Thus, the reaction of **1** with 4,4′-dimethyl-2,2′-bipyridyl (Me_2bpy) was conducted on the grounds that the methyl substituents would give a clear spectroscopic handle. The low-temperature ^1H and $^{13}C\{^1H\}$ NMR spectra of $[Ru(dppe)(CO)(H_2O)(Me_2bpy)][OTf]_2$, **6a** (recorded at 258 K to prevent isomerization), showed only a single methyl signal as expected for a symmetrical arrangement of the two pyridyl rings. Isomerization of **6a** to **6b** occurred upon warming to room temperature to give two methyl resonances, which were characterized in both the ^1H and $^{13}C\{^1H\}$ NMR spectra. The latter also showed a carbonyl signal at δ 199.4 split into a triplet ($J_{CP} = 16.1$ Hz), indicating that it is cis to the dppe ligand (Scheme 1).

Synthesis and X-ray Characterization of [Ru(dppe)(CO)(OTf)(Me$_2$bpy)][OTf] (7). The coordinated water ligand in **6b** proved to be labile and hence dissolution in $CDCl_3$ afforded $[Ru(dppe)(CO)(OTf)(Me_2bpy)][OTf]$ (**7**).[18] The ^{19}F NMR spectrum showed two signals in a 1:1 ratio at −78.97 and −79.07 ppm for coordinated and uncoordinated triflate, respectively. Complex **7** rapidly precipitated from solution, preventing full characterization by NMR spectroscopy. However, the structure of **7** has been unambiguously established using X-ray crystallography. Figure 4 reveals the contents of the asymmetric unit, while selected bond lengths and angles are given in Table 5. The geometry about the ruthenium center in **7** is largely dictated by the steric demands of the chelating bipyridyl ligand (N(1)−Ru−N(2) = 76.73(7)°).[19] This results in severe distortion away from a regular octahedral geometry as shown by the P(2)−Ru−P(1), C(27)−Ru−N(2), and C(27)−Ru−O−(2) angles (85.17(2)°, 171.96(8)°, and 99.48(8)°, respectively).

There are large differences in the Ru−N(1) (2.126(2) Å) and Ru−N(2) (2.267(2) Å) distances of **7**. The notable lengthening of the latter bond arises from differing trans

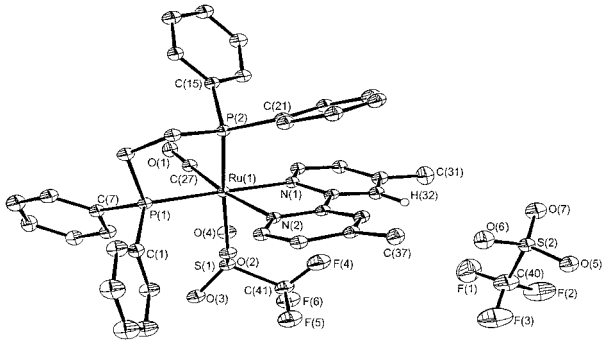

Figure 4. ORTEX diagram of $[Ru(dppe)(CO)(OTf)(Me_2bpy)][OTf]$ (**7**). Thermal ellipsoids are shown at the 30% level.

Table 5. Selected Bond Lengths [Å] and Angles [deg] for $[Ru(dppe)(CO)(OTf)(Me_2Bpy)][OTf]$ (**7**)

Ru(1)−C(27)	1.869(2)	Ru(1)−O(2)	2.212(2)
Ru(1)−N(1)	2.126(2)	Ru(1)−P(2)	2.2826(6)
Ru(1)−N(2)	2.267(2)	Ru(1)−P(1)	2.3392(5)
C(27)−Ru(1)−N(1)	96.25(8)	N(2)−Ru(1)−P(2)	86.35(5)
C(27)−Ru(1)−N(2)	171.96(8)	O(2)−Ru(1)−P(2)	169.85(5)
N(1)−Ru(1)−N(2)	76.73(7)	C(27)−Ru(1)−P(1)	84.33(7)
C(27)−Ru(1)−O(2)	99.48(8)	N(1)−Ru(1)−P(1)	179.11(5)
N(1)−Ru(1)−O(2)	85.26(6)	N(2)−Ru(1)−P(1)	102.74(5)
N(2)−Ru(1)−O(2)	84.00(6)	O(2)−Ru(1)−P(1)	93.98(4)
C(27)−Ru(1)−P(2)	90.50(7)	P(2)−Ru(1)−P(1)	85.17(2)
N(1)−Ru(1)−P(2)	95.60(5)		

(18) Triflate was also found to displace water from **5b** to afford [Ru(dppe)(CO)(OTf)(bpy)][OTf] in $CDCl_3$.

(19) (a) Anderson, P. A.; Deacon, G. B.; Haarmann, K. H.; Keene, F. R.; Meyer, T. J.; Reitsma, D. A.; Skelton, B. W.; Strouse, G. F.; Thomas, N. C.; Treadway, J. A.; White, A. H. *Inorg. Chem.* **1995**, *34*, 6145. (b) Eskelinen, E.; Haukka, M.; Venäläinen, T.; Pakkanen, T. A.; Wasberg, M.; Chardon-Noblat, S.; Deronzier, A. *Organometallics* **2000**, *19*, 163.

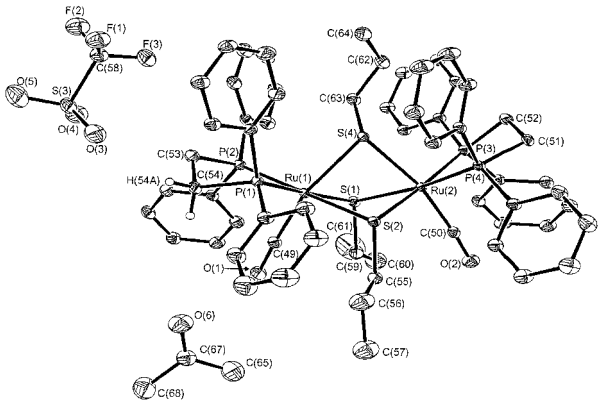

Figure 5. ORTEX diagram of [{Ru(dppe)(CO)}$_2$(μ-SCH$_2$CH$_2$CH$_3$)$_3$][OTf] (**8**). Thermal ellipsoids are shown at the 30% level.

influences of the phosphine (P1) and carbonyl ligands (C27). This is further apparent from the significant differences in the Ru−P(1) and Ru−P(2) bond distances (2.3392(5), 2.2826(6) Å, respectively). There appears to be a weak intramolecular interaction between a phenyl C−H and the coordinated triflate group (C(8)−H(8)···O(3), 3.396 Å) as well as an intermolecular interaction between C(11)−H(11) and O(5) of a symmetry-related anion in the lattice, at 3.451(3) Å.

Reaction of [Ru(dppe)(CO)(H$_2$O)$_3$][OTf]$_2$ with 1-Propanethiol. Addition of 1-propanethiol (3 equiv) to an acetone/water solution of **1** led to an immediate color change from clear to red. Crystallization of the product mixture gave yellow/orange crystals which were isolated in 32% yield and shown to be the dimeric complex [{Ru(dppe)(CO)}$_2$(μ-SCH$_2$CH$_2$CH$_3$)$_3$][OTf] (**8**) by X-ray crystallography (eq 2).

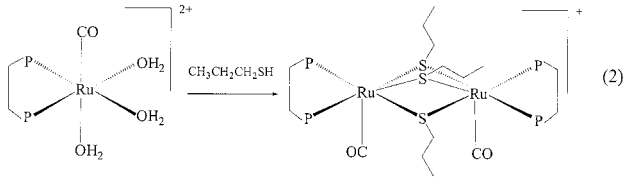

8

The asymmetric unit in **8** (Figure 5) shows the presence of a cationic dinuclear ruthenium(II) core bridged by the sulfur atoms of three thiolate groups. Selected bond distances and angles for **8** are given in Table 6. The Ru−S distances (average 2.463(5) Å) are comparable to those reported in the literature for [{(arene)Ru}$_2$(μ-SPh)$_3$]$^+$ (arene = hexamethylbenzene, *p*-cymene), while there is only small deviation in the Ru−S−Ru angles (average 86.5°) from 90°.[20] However, particularly striking is the distortion away from an octahedral geometry at the ruthenium centers: the angles between the carbonyl ligands and the unique thiolate lying below the plane of the phosphines are 165.56° and 167.22° for Ru(1) and Ru(2), respectively. When viewed along the metal−metal vector, the structure of **8** reveals that the bridging sulfurs are staggered with respect to the phosphorus and carbonyl carbon atoms at both ends of the molecule, reflecting the local octahedral coordination sphere at both metal centers. This highly distorted geometry is exemplified in the angles subtended by the carbonyl carbon and the trans sulfur at each of the ruthenium atoms, which have values of 165.59(7)° and 167.23(6)° for Ru(1) and Ru(2), respectively. The metal−metal distance in **8** is 3.376 Å, which precludes the presence of a Ru−Ru interaction.

Table 6. Selected Bond Lengths [Å] and Angles [deg] for [{Ru(dppe)(CO)}$_2$(μ-SCH$_2$CH$_2$CH$_3$)$_3$][OTf] (**8**)

Ru(1)−C(49)	1.851(2)	Ru(1)−P(1)	2.3340(5)
Ru(1)−P(2)	2.3539(5)	Ru(1)−S(2)	2.4387(5)
Ru(1)−S(1)	2.4662(5)	Ru(1)−S(4)	2.4964(5)
Ru(2)−C(50)	1.861(2)	Ru(2)−P(4)	2.3211(5)
Ru(2)−P(3)	2.3547(5)	Ru(2)−S(2)	2.4473(5)
Ru(2)−S(4)	2.4654(5)	Ru(2)−S(1)	2.4653(5)
C(49)−Ru(1)−P(1)	87.77(6)	C(49)−Ru(1)−P(2)	87.54(7)
P(1)−Ru(1)−P(2)	82.657(18)	C(49)−Ru(1)−S(2)	93.56(7)
P(1)−Ru(1)−S(2)	94.968(17)	P(2)−Ru(1)−S(2)	177.346(17)
C(49)−Ru(1)−S(1)	95.30(6)	P(1)−Ru(1)−S(1)	176.421(18)
P(2)−Ru(1)−S(1)	99.279(17)	S(2)−Ru(1)−S(1)	83.030(16)
C(49)−Ru(1)−S(4)	165.59(7)	P(1)−Ru(1)−S(4)	99.830(17)
P(2)−Ru(1)−S(4)	105.468(17)	S(2)−Ru(1)−S(4)	73.711(16)
S(1)−Ru(1)−S(4)	76.777(16)	C(50)−Ru(2)−P(4)	93.84(6)
C(50)−Ru(2)−P(3)	89.89(6)	P(4)−Ru(2)−P(3)	83.926(17)
C(50)−Ru(2)−S(2)	94.69(6)	P(4)−Ru(2)−S(2)	92.056(17)
P(3)−Ru(2)−S(2)	174.107(17)	C(50)−Ru(2)−S(4)	167.23(6)
P(4)−Ru(2)−S(4)	92.708(17)	P(3)−Ru(2)−S(4)	101.709(17)
S(2)−Ru(2)−S(4)	74.111(16)	C(50)−Ru(2)−S(1)	95.43(6)
P(4)−Ru(2)−S(1)	169.757(17)	P(3)−Ru(2)−S(1)	100.411(17)
S(2)−Ru(2)−S(1)	82.871(16)	S(4)−Ru(2)−S(1)	77.367(16)
Ru(2)−S(1)−Ru(1)	86.412(15)	Ru(1)−S(2)−Ru(2)	87.419(16)
Ru(2)−S(4)−Ru(1)	85.753(15)		

Multinuclear NMR studies of [{Ru(dppe)(CO)}$_2$(μ-SCH$_2$-CH$_2$CH$_3$)$_3$][OTf] in acetone solution are consistent with the solid-state structure. The proton NMR spectrum exhibits two different types of propyl groups in a ratio of 1:2; a significant chemical shift difference ($\Delta\nu$ = 1.1 ppm) exists between the methyl group resonances, with the unique CH_3 appearing at δ −0.23. ^{1}H COSY, ^{1}H−^{13}C HMQC, and HMBC experiments were used to fully assign the $CH_3CH_2CH_2$− signals in both the ^{1}H and ^{13}C{^{1}H} NMR spectra. The reaction of **1** with other thiols does not proceed in a manner similar to the formation of **8**. Both H_2S and $C_6H_{11}SH$ gave mixtures of products that proved impossible to separate and characterize.

Reaction of [Ru(dppe)(CO)(H$_2$O)$_3$][OTf]$_2$ with CO. In contrast to the rapid displacement of the water ligands in **1** by strongly coordinating groups such as acetonitrile or DMSO, the reaction of **1** with CO (1 atm) proceeded very slowly with complete conversion to a single, new ruthenium-containing complex taking place over 3 weeks at room temperature. This product was assigned as the cationic tricarbonyl hydride complex [Ru(dppe)(CO)$_3$H][OTf] (**9**), due to the presence of three carbonyl bands in the IR spectrum (2110, 2062, and 2051 cm^{-1})[21] and a triplet resonance at δ −7.57 (J_{HP} = 17.80 Hz) in the ^{1}H NMR spectrum. The spectroscopic data are consistent with a fac arrangement of the CO ligands and are in good agreement with that reported by Gladfelter et al. for the PF_6 salt of **9**, which was

(20) (a) Dev, S.; Mizobe, Y.; Hidai, M. *Inorg. Chem.* **1990**, *29*, 4797. (b) Schacht, H. T.; Haltiwanger, R. C.; DuBois, M. R. *Inorg. Chem.* **1992**, *31*, 1728. (c) Mashima, K.; Mikami, A.; Nakamura, A. *Chem. Lett.* **1992**, *241*, 1795.

(21) Skoog, S. J.; Jorgenson, A. L.; Campbell, J. P.; Douskey, M. L.; Munson, E.; Gladfelter, W. L. *J. Organomet. Chem.* **1998**, *557*,13.

Scheme 2

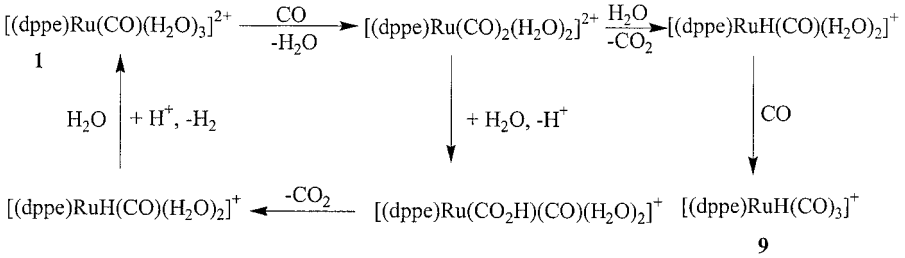

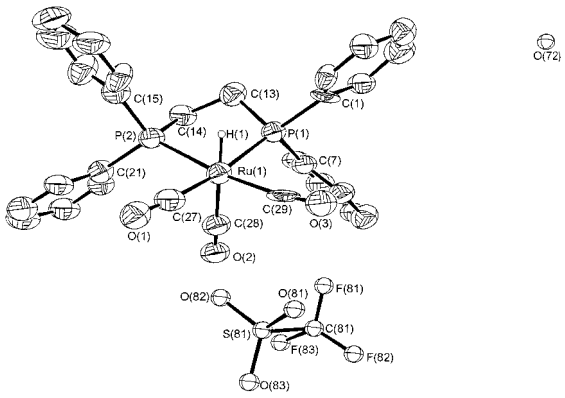

Figure 6. ORTEX diagram of $[Ru(dppe)(CO)_3H][OTf]$ (**9**). Thermal ellipsoids are shown at the 30% level.

synthesized upon hydrogen atom abstraction from Bu_3SnH by the radical cation $[Ru(dppe)(CO)_3]^+$.[22] We were unable to successfully isolate **9** from the reaction mixture, partly due to its apparent instability in solution in the absence of CO. However, we have prepared the complex independently by protonation of $Ru(dppe)(CO)_3$ with triflic acid under a CO atmosphere. Thus, an X-ray structure determination has been performed on this complex, although the poor quality of the crystals and disorder in the triflate anion prevented the structure from being solved with the same high degree of accuracy as for the other compounds reported in this paper. Nevertheless, the stereochemistry at the ruthenium center was established beyond doubt and is illustrated in Figure 6. The fac arrangement of the CO ligands imposed by the chelating phosphine ligands contrasts with the mer geometry in the structure of $[Ru(PPh_3)_2(CO)_3H]^+$ previously reported.[23]

The formation of $[Ru(dppe)(CO)_3H][OTf]$ from reaction of **1** with CO was also probed by ^{13}CO labeling. Monitoring by $^{31}P\{^1H\}$ NMR spectroscopy showed the appearance after 3 days of an initial product believed to be $[Ru(dppe)(CO)_2(H_2O)_2][OTf]_2$, which displayed two doublets of doublets at δ 64.5 (J_{PC} = 9.3 Hz, J_{PP} = 14.0 Hz) and 42.8 (J_{PC} = 102.3 Hz, J_{PP} = 14.0 Hz). The size of the P−C coupling constants indicates substitution of water at an equatorial site by ^{13}CO. The $^{13}C\{^1H\}$ NMR spectrum showed a single ^{13}C-enhanced carbonyl resonance at δ 187.0 with coupling to two inequivalent ^{31}P nuclei.

The ^{31}P signals from $[Ru(dppe)(CO)_2(H_2O)_2][OTf]_2$ diminished over weeks at room temperature and were replaced by a signal for **9**, showing coupling to ^{13}CO. In addition to two CO resonances for **9**, the $^{13}C\{^1H\}$ NMR spectrum indicated incorporation of ^{13}CO into residual amounts of **1**, but, most importantly, displayed a signal for $^{13}CO_2$ at δ 126.3. The formation of **9**, ^{13}CO incorporation into **1**, and evolution of CO_2 can all be rationalized by a mechanism based on nucleophilic attack by water on a coordinated CO ligand in **1** leading to a water gas shift reaction. A postulated pathway is shown in Scheme 2.[24]

Thus, the formation of **9** constitutes the trapping of an intermediate on the cycle by addition of excess CO. This is confirmed by the observation that reaction of $[Ru(dppe)(^{12}CO)_3H][OTf]$ with ^{13}CO results in incorporation of the label, but does not yield $^{13}CO_2$.

A number of recent examples of water gas shift chemistry involving electrophilic non-phosphine stabilized ruthenium carbonyl complexes have been reported.[25] In most of these cases, the isolation of hydrido complexes has proved elusive, although Fachinetti and co-workers have been able to trap $[Ru(H_2O)_3(CO)_2H]^+$ with either pyridine or ethene to give $[Ru(py)_3(CO)_2H]^+$ and $[Ru(H_2O)_3(CO)_2(C_2H_5)]^+$ respectively.[26]

The discovery of a water gas shift mechanism as a pathway toward production of **9** prompted us to reinvestigate the formation of **1**, which occurs via substitution of CO and triflate in $Ru(dppe)(CO)_2(OTf)_2$ upon addition of water.[8] Thus, addition of water to a chloroform solution of partially ^{13}CO labeled $Ru(dppe)(CO)_2(OTf)_2$ resulted in the formation of $^{13}CO_2$, implying that nucleophilic attack of water on a coordinated CO in the bis-triflate complex is also responsible for the formation of **1**.

Conclusions

Substitution of one, two, or all three water ligands in $[Ru(dppe)(CO)(H_2O)_3][OTf]_2$ by a range of donor ligands has been demonstrated to result in the formation of both mononuclear and dinuclear ruthenium products. In all cases, we have shown, at least qualitatively, that initial substitution of the equatorial water ligands (trans to dppe) occurs. This is in agreement with kinetic studies on *trans*-$[Ru(NH_3)_4$-

(22) Sherlock, S. J.; Boyd, D. C.; Moasser, B.; Gladfelter, W. L. *Inorg. Chem.* **1991**, *30*, 3626.
(23) Siedle, A. R.; Newmark, R. A.; Gleason, W. B. *Inorg. Chem.* **1991**, *30*, 2005.
(24) Ford, P. C.; Rokicki, A. *Adv. Organomet. Chem.* **1988**, *28*, 139.
(25) (a) Fachinetti, G.; Funaioli, T.; Lecci, L.; Marchetti, F. *Inorg. Chem.* **1996**, *35*, 7217. (b) Lavigne, G. *Eur. J. Inorg. Chem.* **1999**, 917. (c) Faure, M.; Maurette, L.; Donnadieu, B.; Lavigne, G. *Angew. Chem., Int. Ed.* **1999**, *38*, 518. (d) Funaioli, T.; Cavazza, C.; Marchetti, F.; Fachinetti, G. *Inorg. Chem.* **1999**, *38*, 3361. (e) Hill, A. F. *Angew. Chem., Int. Ed.* **2000**, *39*, 130.
(26) Fachinetti, G.; Funaioli, T.; Marchetti, F. *J. Organomet. Chem.* **1995**, *498*, c20.

$(H_2O)(PR_3)]^{2+}$ which have established that the kinetic trans effect of dppe is much greater than that of CO.[27]

The triflate anion appears to play an important role in the reactivity of **1**.[28] While hydrogen bonding interactions have been reported to help stabilize many organometallic aqua complexes, we find that OTf also plays the role of hydrogen bond acceptor in weak C−H···O hydrogen bonding interactions in the solid-state structures of **2**, **3**, and **4**. Dissolution of [Ru(dppe)(CO)(H_2O)(Me_2bpy)][OTf]$_2$, **6b**, in nonprotic solvents results in triflate playing an even more interactive role in substituting water to afford **7**. We are currently engaged in studies which compare the role of triflate with that of other anions (BF_4, SbF_6, NTf) in influencing the chemistry of **1**.

Water gas shift chemistry has been shown to be important in both the mechanism of formation of **1** (from Ru(dppe)-$(CO)_2(OTf)_2$) and in its reaction with CO, which yields the cationic hydride complex $[Ru(dppe)(CO)_3H]^+$. Additional work is required to see if this underlying pathway can be utilized further.

Acknowledgment. We thank EPSRC and the University of Bath for financial support. We acknowledge JREI/EPSRC for funding the CCD X-ray diffractometer and Johnson Matthey plc for the loan of $RuCl_3 \cdot xH_2O$. We gratefully acknowledge the comments from a referee on an earlier version of this paper who instigated our study of the water gas shift chemistry associated with **1**.

Supporting Information Available: Analytical and X-ray crystallographic data including tables of atomic coordinates, bond lengths and angles, anisotropic displacement parameters, hydrogen coordinates and U_{eq}, and packing diagram. This material is available free of charge via the Internet at http://pubs.acs.org.

IC020029Z

(27) Franco, D. W. *Coord. Chem. Rev.* **1992**, *119*, 199.
(28) (a) Lawrance, G. A. *Chem. Rev.* **1986**, *86*, 17. (b) Beck, W.; Sünkel, K. *Chem. Rev.* **1988**, *88*, 1405.